European Review for Medical and Pharmacological Sciences 2023; 27: 275-290

Identification of a chromatin regulator signature for predicting prognosis of prostate cancer patient

W.-B. LIAO[1], L. LIU[2]

[1]Urology Department, Renmin Hospital of Wuhan University, Wuhan, China
[2]Urology Department, Banan Hospital of Chongqing Medical University, Chongqing, China

Abstract. – OBJECTIVE: Prostate cancer is a malignancy with unsatisfactory prognosis. Mounting proofs have verified that chromatin regulators (CRs) participate in the developmental process of tumor. Hence, this research intended to reveal the biofunction and prognosis significance of CRs in prostate cancer patients.

MATERIALS AND METHODS: CRs were obtained from previously finished topic research. The mRNA expression and clinical data were acquired from TCGA and GEO datasets. Molecular subtypes were identified by ConsensusClusterPlus package. Cox regressive analyses, LASSO regressive analyses and stepAIC were utilized to screen the prognosis-related genes and establish the risk model for forecasting outcomes in prostate cancer. Genomic variation, immune infiltration, drug sensitivity difference and analysis of clinical features were all investigated.

RESULTS: 462 samples in TCGA cohort study were classified into two clusters base on 23 prognosis CRs. Patients in cluster 1 (clust1) presented better overall survival (OS), lower tumor mutation burden (TMB), enhanced immune infiltration, higher immune escape and hyposensitivity to several drugs. Furthermore, our team smoothly established and substantiated a 10 CR-derived model for forecasting the prognostic results of individuals with prostate cancer, which was an independent prognosis indicator. Functional analyses revealed that CRs were predominantly enriched in tumor-associated signal paths. The CR-derived model was related to immunocyte infiltration and sensitive to several drugs.

CONCLUSIONS: Holistically, the present research offered fresh enlightenment regarding the biofunction of CRs in prostate cancer. Our team discovered a dependable prognosis marker for the survival of individuals with prostate cancer.

Key Words:
Chromatin regulators, Molecular subtypes, Prostate cancer, The Cancer Genome Atlas, Signature, Prognosis.

Introduction

Prostate carcinoma is one of the most common diagnosed tumors in males and is particularly common in developing nations[1]. About 15% of prostate cancer cases are high-risk and potentially fatal[2]. Although radical therapies like prostate excision and radiation treatment have been successful in prostate cancer, there are still problems like determination and localization of prostate lesions, that remain to be solved[3,4]. To ameliorate the survival and quality of prostate carcinoma sufferers, further research is needed to personalize treatment, which depends on the knowledge of the developmental process of prostate cancer.

Chromatin regulators (CRs) are indispensable regulatory elements in epigenetics[5]. In healthy mammalian cells, chromatin architecture is modulated by epigene events, like heritable DNA CpG methylation and histone modifications and chromatin remodeling, which ensures normal genetic expressions in reaction to different bio-signals[6]. During tumorigenesis, abnormal regulation of epigene mechanisms induces abnormal chromatin conformation and aberrant stimulation or silencing of genes that control cellular development and death, hence facilitating tumorigenesis and developmental process[7-9]. CRs have been shown to be aberrantly expressed and correlated to prognosis in different tumor types. HMGA1 is on the short arm of human chromosome 6 (6p21), a region participating in chromosome abnormities related to mankind tumors. An elevation of the expressing level of HMGA1 is related to high grade cancers and advanced prostate cancer, overexpressed HMGA1 in prostate cancer lineage cells induced chromosomal unsteadiness and structure abnormities[10,11]. In prostate cancer, histone demethylase KDM7A controls androgen receptor activity and tumor growth[12]. EZH2, a histone lysine methyl-

Corresponding Author: Lang Liu, MD; e-mail: liulang19930630@163.com

transferase, participated in different malignancy phenotypes like programmed cell death and metastases in prostate cancer[13].

In the present paper, our team highlighted the expression profile of CRs in prostate cancer and their prognostic value through bioinformatics analysis. We intended to construct and demonstrate a prognosis marker on the basis of CRs that can validly forecast the prognosis of individuals with prostate cancer. Moreover, our team explored the association between the prognostic features of prostate cancer and the immune micro-environment, which provides a theory-wise foundation for immuno-checkpoint treatment regimens.

Materials and methods

Raw Data Acquisition

Public prostate cancer RNA-seq data, clinicopathological characteristics, and mutation data (CNV and SNP) were acquired from TCGA database[14] and GEO database[15] (GSE116918). In total, 462 tumor and 52 normal specimens in the TCGA-prostate cancer cohort and 248 tumor specimens in the GSE116918 cohort were utilized for analyses. An overall 870 CRs were acquired from previously finished topic researches[5].

Cluster Analysis

As per the standards of |logFC| >1 and FDR < 0.05, CRs with differential expression were determined *via* limma package of R program. Next, above differentially expressed CRs were studied *via* univariable Cox analysis through the Coxph function of R package survival in TCGA dataset, and $p < 0.05$ was considered the liminal value. Then, molecular typing was performed separately for TCGA dataset samples *via* the R package Consensus Cluster Plus 1.52.0[16]. Pam arithmetic and "Pearson" distance were utilized to complete 500 bootstraps with every bootstrap having specimens (≥ 80%) of TCGA dataset. Cluster number k was between 2 and 10, and the optimum k was identified as per cumulative distribution function (CDF) and AUC. The clustering was substantiated in GSE116918 dataset. Survival curves (KM curves) between molecular subtypes were then analyzed for difference. In addition, differences in the distribution of clinical characteristics between molecular subtypes were compared and a Chi-square test was completed; $p < 0.05$ had significance on statistics.

Mutation Analysis

Waterfall plot was generated to explore the detailed single-nucleotide variant (SNV) characteristics between molecular subtypes *via* "oncoplot" function in R software, "maftools" package[17].

Cell-type Identification by Estimating Relative Subsets of RNA Transcripts (CIBERSORT)

CIBERSORT analyses were utilized to compare diversities in different immunocytes in molecular subtypes. Wilcox.test analyses were completed to identify the difference of 22 kinds of infiltrating immunocyte score between molecular subtypes. The "ggplot2" package[18] was used to realize the visualization of the distributional status of the diversities in 22 kinds of infiltration immunocytes.

Computation of Immune Score, Stromal Score, and Estimate Score

R software ESTIMATE arithmetic[19] was utilized to compute overall stroma level (Stromal Score), the immunocyte infiltration (Immune Score) and the combination (ESTIMATE Score) of sufferers in the TCGA-prostate cancer cohort using Wilcox.test analysis to determine difference between molecular subtypes.

Tumor Immune Dysfunction and Exclusion (TIDE)

TIDE[20,21] is a calculation framework designed to assess the potential of cancer immunoescape from the genetic expression profiles of tumor specimens. TIDE was used to predict sample responses in the TCGA-prostate cancer datasets, and to compare the proportion of treatment responses in different subtypes, as well as TIDE scores.

Drug Sensitivity Analysis

pRRophetic[22] was used to predict the sensitivity of erlotinib, sunitinib, paclitaxel, VX-680, TAE684 and crizotinib to IC50 in molecular subtypes.

Establishment and Corroboration of a Prognosis Model on the Basis of CRs

Our team completed univariable Cox regressive analyses to identify the prognosis significance of CRs. Then lasso-penalized Cox regressive analyses were leveraged to establish the prognosis risk model *via* the glmnet R package. Risk scoring was computed *via* the equation below:

$$Risk\ Score = \sum_{i=1}^{n} Coefficient\ (mRNAi) \times Expression\ (mRNAi)$$

where Coefficient is lasso Cox regressive model coefficient of the relevant mRNA. Our team separated prostate cancer sufferers into $risk_{high}$ and $risk_{low}$ groups as per the mid-value of risk scoring. Survival analyses were completed *via* the Kaplan-Meier (K-M) curve to assess the prognoses. Time-associated ROC analyses were utilized to analyze the prognosis significance of our modeling method through the survival ROC package. GSE116918 data set was deemed as the verified set for further validating the prognosis value of the modeling method. In addition, diversities in the distributional status of clinical characteristics between these two groups were compared and a Chi-square test was utilized; $p < 0.05$ had significance on statistics.

A predictive Nomogram was Developed

Univariable cox regressive analyses were completed to identify the association between age, T Stage, N Stage, Cluster and Risk Score. Clinical factors which could forecast the prognoses in an independent manner were identified *via* multivariable cox regressive survival analyses as per Hazard ratio (HR), 95% CI and *p*-value. Clinical variables and the CR-derived hallmark risk scoring were utilized to construct a nomograph related to the outcomes for assessing the possibility of 1-, 3-, and 5-year OS for prostate cancer sufferers. The concordance index (C-index) and correction curve were utilized to analyze the prediction capability of the nomograph.

Statistical Analysis

The R program 4.0.3 was utilized for statistic assay. K-M curves were utilized for analyzing survival status *via* the Survminer R package 2.43-3. $p<0.05$ had significance on statistics (*$p<0.05$; **$p<0.01$; ***$p<0.001$; ****$p<0.0001$).

Results

Construction of CRs-Related Subtypes

Limma package was used to analyze DEGs between tumor and healthy specimens in TCGA cohort study, and 756 up-regulated and 1,199 down-regulated genes were discovered (Figure 1A). Among them, 58 genes belonged to CRs (Figure 1B). 23 prognosis factors were determined *via* univariable cox survival analyses (Figure 1C), and they were closely correlated (Figure 1D).

Based on 23 prognostic factors, 462 samples in TCGA cohort study were classified into two clusters using ConsensusClusterPlus package (Figure 2A-C). KM survival curve results revealed that sufferers in clust1 had a better survival duration compared to clust2 in TCGA cohort study and GSE116918 dataset (Figure 2D, E). Of the distributional status of two clusters in diverse clinical characteristics, remarkable diversity in Event in TCGA cohort study were observed (Figure 3).

Functional Enrichment Analysis of CRs-Related Subtypes

To better reveal the value of our sub-types, the function enrichment was analyzed. First, 154 significance pathways between two clusters were obtained using GSVA package (Figure 4A). GSEA analysis in ClusterProfiler package displayed that the majority of pathways were stimulated in clust1: for example, enrich score of ALLOGRAFT_REJETION were higher in clust1 than that in clust2; moreover, this pathway also activated in clust1(Figure 4B).

Analysis of Genomic Variation in CRs Related Subtypes

Genomic variation between two clusters were analyzed in TCGA cohort study. Firstly, we extracted molecular genetic characteristics, including Aneuploidy Score, Nonsilent Mutation Rate, Fraction Altered, Number of Segments and Homologous Recombination Defects, the results showed that those characteristics were higher in cluster2 than in cluster1 (Figure 5A). Moreover, our team identified the top 15 mutation genes based on SNV data using maftools software (Figure 5B). *TP53* and *SPOP* are two top mutation genes in which missense variants facilitated the majority of SNVs.

Immune Infiltration Level Analysis and Drug Sensitivity Analysis in two Clusters

Next, we evaluated the speculated percentage of 22 immunocytes in 2 clusters in TCGA dataset. 8 kinds of immunocytes with significantly different distributions between two clusters were found (Figure 6A). Surprisingly, clust1 had higher score of StromalScore, ImmuneScore and ESTIMATEScore (Figure 6B). Our team afterwards

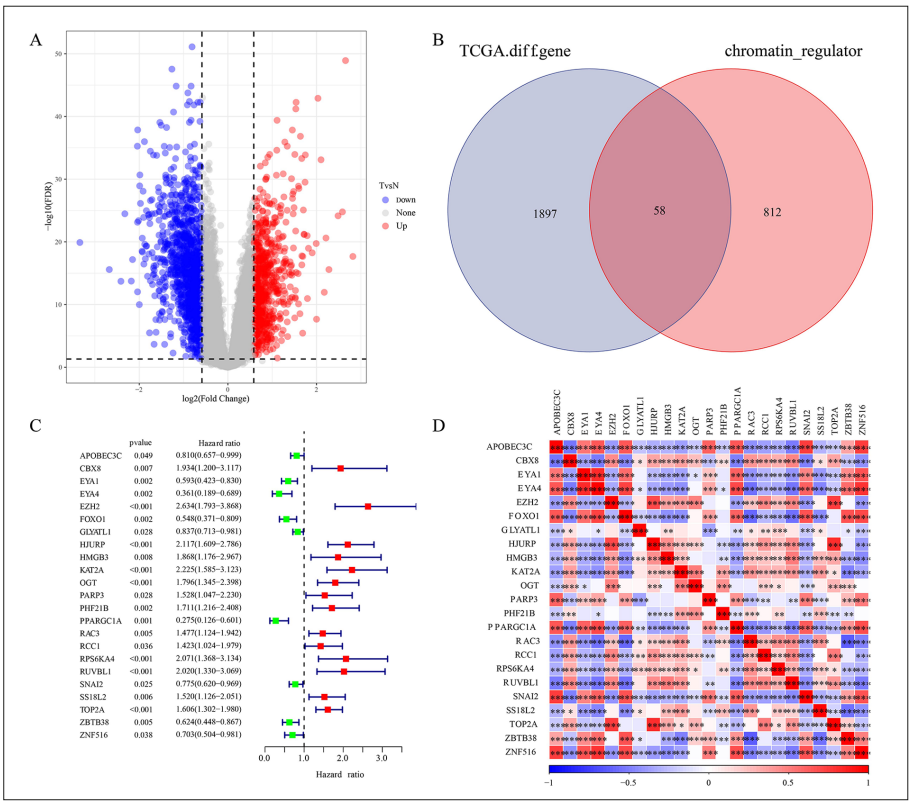

Figure 1. Determination of chromatin regulators with differential expression. **A**, DEGs between prostate carcinoma and para-carcinoma tissue in TCGA dataset. **B**, Venn of differentially expressed genes and chromatin regulators. **C**, Forest map of significant prognostic chromatin regulators. **D**, Heatmap of significant prognostic chromatin regulators.

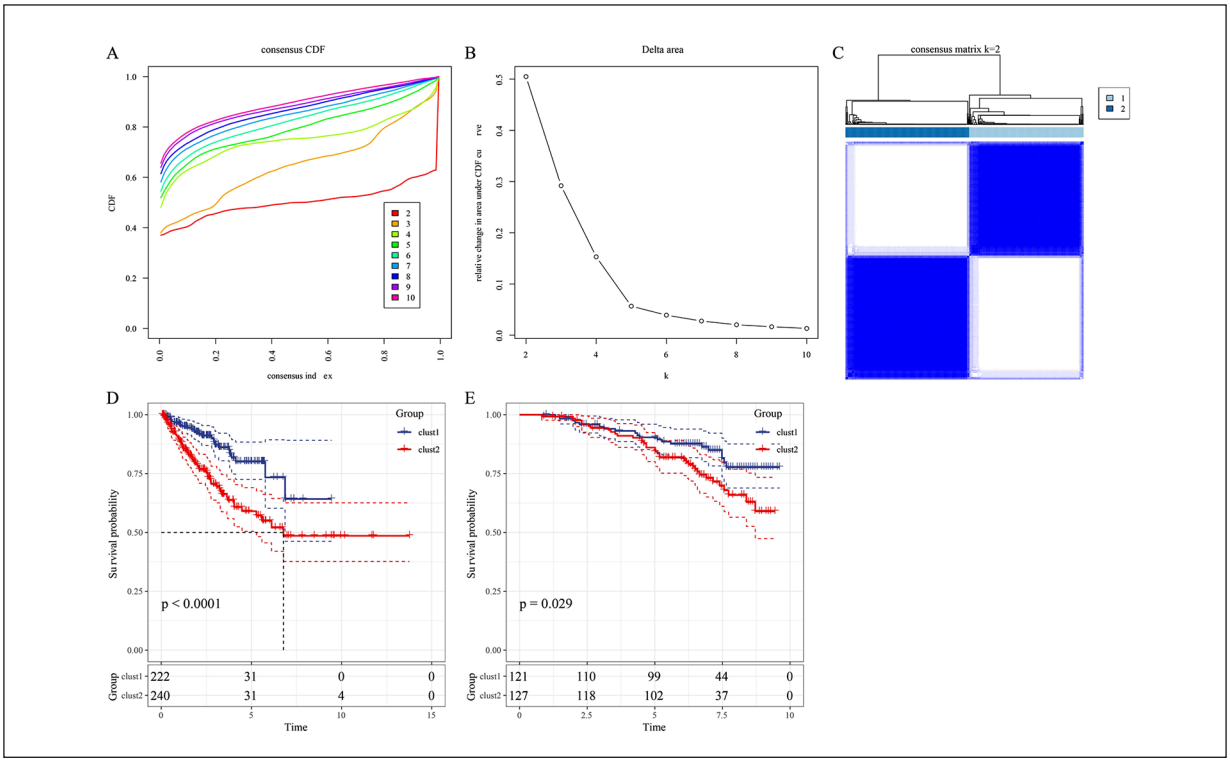

Figure 2. Identification of chromatin regulators associated molecular subtypes. **A**, CDF curve of patients in TCGA dataset when K=2-10. **B**, CDF delta area when K=2-10. **C**, ConsensusClusterPlus identifies two chromatin regulators associated molecule sub-types. **D**, K-M curve between C1 and C2 sub-types in TCGA cohorts. Log-rank test was utilized. **E**, K-M curve between C1 and C2 sub-types in GSE116918 dataset. Log-rank test was utilized.

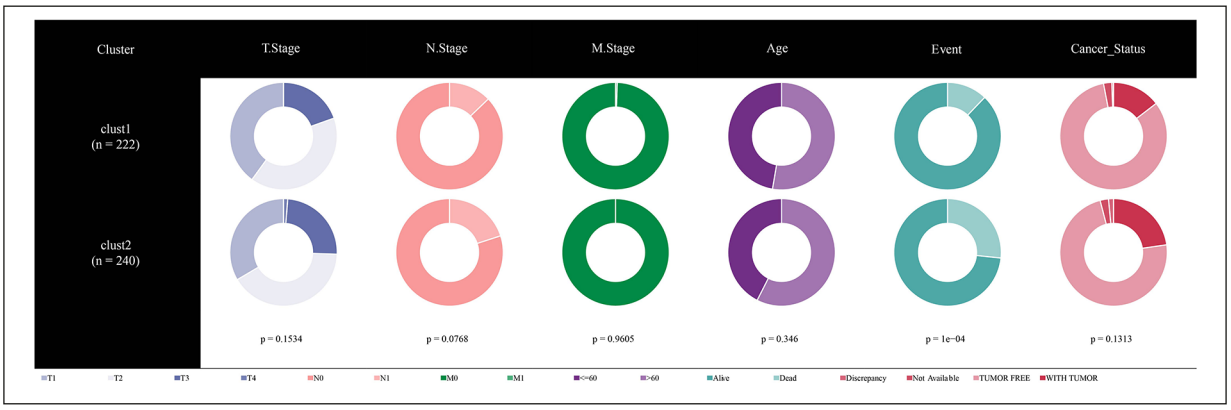

Figure 3. The distributional status of diverse clinical characteristics in C1 and C2 sub-types, which involved T stage, N stage, M stage, and Age, Event and cancer status. Chi-square test was utilized.

evaluated the 10 enriched oncogenesis pathways and discovered that 8 of 10 oncogenesis pathways were enriched in a differential manner between two clusters (Figure 6C).

Moreover, the forecasted scores of immune therapy biomarkers were computed *via* the TIDE arithmetic. TIDE and IFNG were greater in clust1 group *vs.* clust2 group (Figure 6D). Our team assessed the qualities of TIDE T cell function disorder scores, which were also higher in clust1 group (Figure 6D). T cell exclusion, as well as two cellular types discovered to suppress T cell infiltration in cancers [i.e., myeloid-derived suppressor cells (MDSC) and the M2 subtype of tumor-associated macrophages (TAM. M2)], were all higher in clust1 group (Figure 6D). Those outcomes indicated that sufferers in clust2 were better candidates for immunotherapy.

To ameliorate the treatment efficacy of sufferer prostate cancer, our team explored the susceptibility diversity of commonly seen chemo medicines amongst the two groups. The outcomes of GDSC database analyses revealed that the IC50 results of medicines like Erlotinib, Sunitinib, Paclitaxel, VX-680, TAE684 and Crizotinib were higher in patients of cluster2 than those of cluster1, which unveiled that sufferer in the Cluster2 were remarkably more susceptible to those medicines (Figure 6E).

Construction and Corroboration of CR-Derived Signature

An overall 981 CRs, which involved 81 CRs with downregulation and 901 CRs with upregulation, were determined as CRs with differential expression between two clusters in the TCGA dataset (Figure 7A), of which 778 genes belonged to tumor key genes (Figure 7B). Based on 778 CR, our team utilized univariable Cox regressive analyses to investigate the prognosis merit of CR. The outcome revealed that 245 of them exhibited prognosis significance.

Afterwards, LASSO Cox regressive analyses and stepAIC were utilized to establish a prognosis hallmark for prostate cancer sufferers. A risk model was smoothly developed using 10 genes (*FCER1A*, *ZFP36L2*, *LAPTM4B*, *TRIM2*, *SLC22A3*, *SCUBE2*, *LCN2*, *PAQR6*, *NOXA1* and *CDC20*) (Figure 7C, D). The risk scoring was computed *via* the coefficients of 10 CRs according to the following equation: risk score = (0.522***FCER1A* expression) + (0.309***ZFP36L2* expression) + (0.365***LAPTM4B* expression) - (0.359***TRIM2* expression) - (0.143***SLC22A3* expression) + (0.235***SCUBE2* expression) - (0.347***LCN2* expression) + (396***PAQR6* expression) + (0.4***NOXA1* expression) + (0.449* *CDC20* expression).

Patients were classified into $risk_{high}$ and $risk_{low}$ groups as per the mid-value of risk scoring. The mortality rates of $risk_{high}$ sufferers were remarkably greater *vs.* $risk_{low}$ sufferers in TCGA dataset ($p < 0.0001$) (Figure 8A) and GSE116918 dataset ($p < 0.0001$) (Figure 8C). The time-reliant ROC analyses revealed that the prognosis accurateness of the CR-derived hallmark was 0.83, 0.83 and 0.8 at 1-, 3-, 5-year separately in the TCGA dataset (Figure 8B) and 0.95, 0.79 and 0.79 at 1-, 3-, 5-year separately in the GSE116918 dataset (Figure 8D).

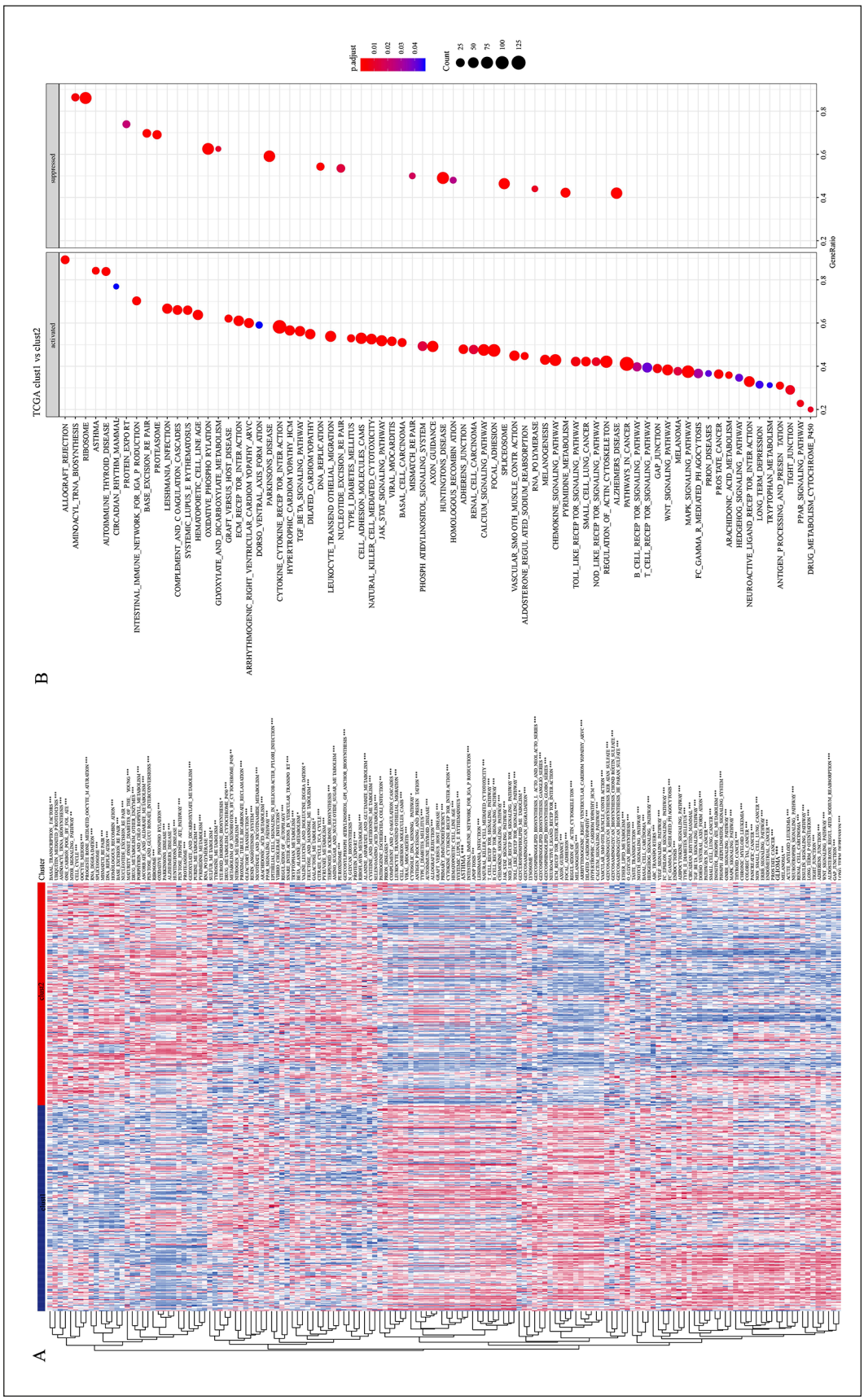

Figure 4. Functional enrichment analysis of two clusters. **A**, GSVA analysis identified significant pathways in two clusters in TCGA dataset. **B**, GSEA analysis identified significant pathways in two clusters in TCGA dataset.

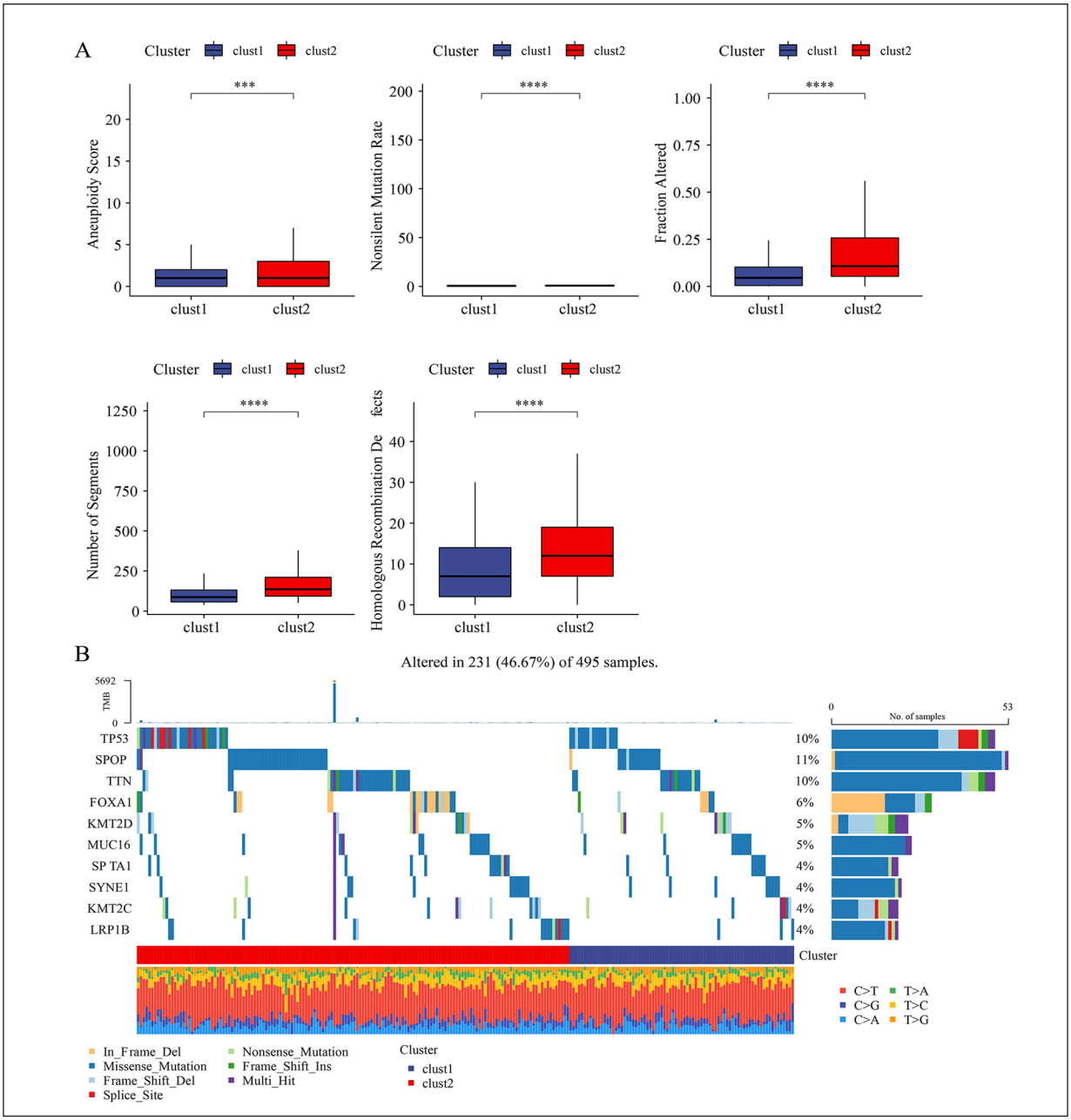

Figure 5. Genomic variation between two clusters were analyzed in TCGA cohort study. **A**, Aneuploidy Score, Nonsilent Mutation Rate, Fraction Altered, Number of Segments and Homologous Recombination Defects, were higher in cluster2 than those in cluster1. **B**, The top 15 mutated genes between two clusters.

Relationship Between the CR-Derived Signature and Clinical Features

The result (Figure 9A) revealed that remarkable diversities existed between $risk_{high}$ and $risk_{low}$ sufferers in Cluster (p=0.0011), T stage (p=0.0109), N stage (p=0), Age (p=0.015), Event (p=0) and Cancer status (p=0) but no remarkable diversities existed in M stage (p=1). In addition, stratified analyses were completed to explore the prognosis merit of the hallmark in sub-groups. This study discovered that the CR-derived hallmark exhibited splendid ability in forecasting prognoses in clust1 *vs.* clust2, N0 *vs.* N1, age > 60 *vs.* age <=60, T1-T4 stage, Alive *vs.* Death, Cancer status, except M0 *vs.* M1 (Figure 9B).

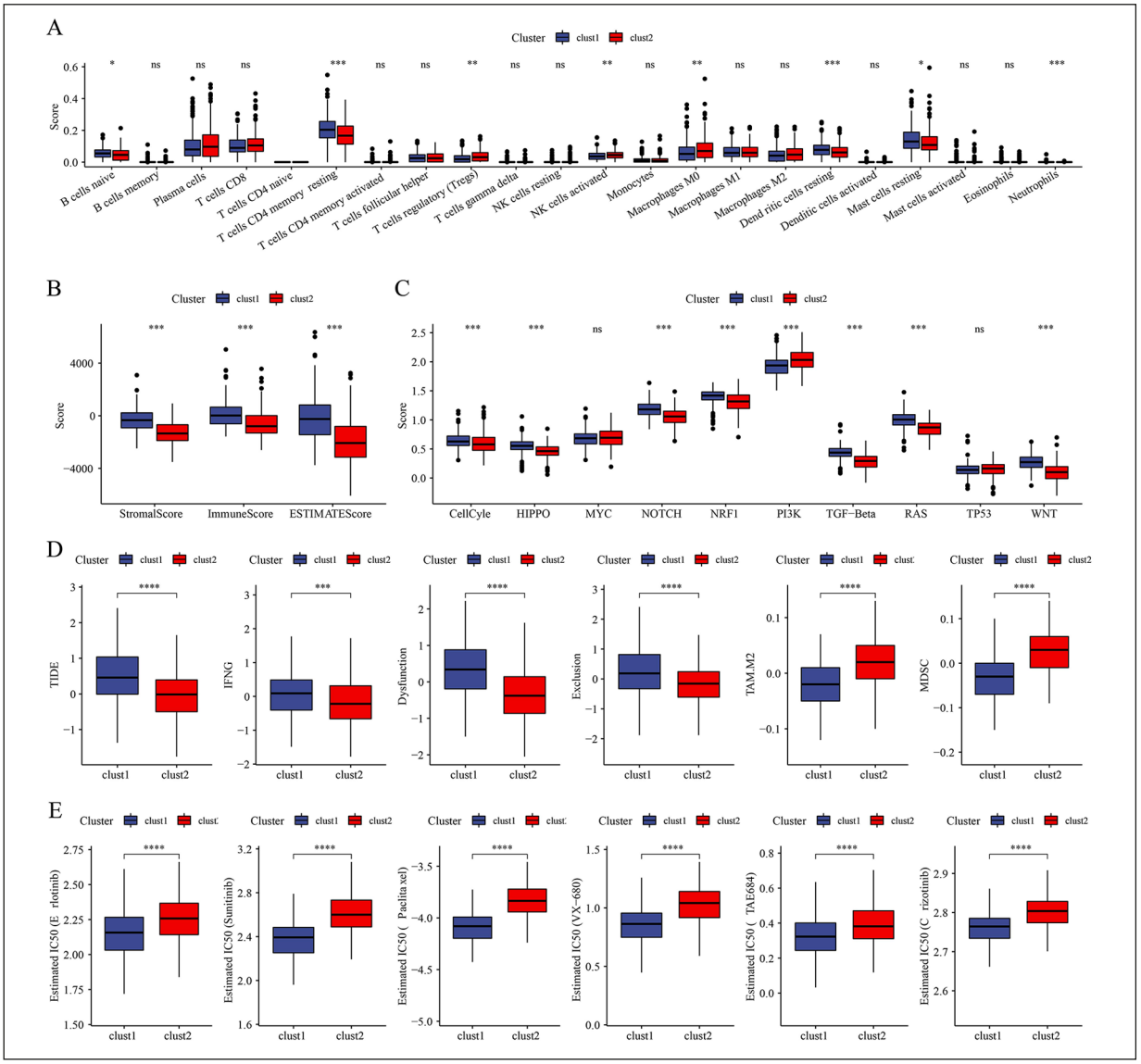

Figure 6. Depiction of TME and immunotherapy between two sub-types in TCGA dataset. **A**, Enrichment of 22 immunocytes assessed *via* CIBERSORT. **B**, ESTIMATE approach for computing stroma scoring and immunity scoring. **C**, Differences of 10 oncogenic pathways score between two clusters in TCGA dataset. **D**, TIDE scoring, IFNG scoring, T cell dysfunction disorder scoring, T cell exclusion scoring, MDSC and TAM.M2 scoring of C1 and C2 sub-types in TCGA dataset. **E**, GDSC database analyses revealed that the IC50 results of medicines like erlotinib, sunitinib, paclitaxel, VX-680, TAE684 and crizotinib were higher in patients in clust2 than in those in clust1.

Pathways Characteristics of CR-based Signature

In order to better study the potential regulatory pathways of signature, enrichment scoring of every pathway was computed *via* the GSVA package of R language, and the correlation between risk scoring and enrichment scores of pathways was analyzed by Rcorr function of Hmisc package. The outcome revealed that 9 pathways were remarkably related to signature (Figure 10A). Among them, 3 pathways were positively correlated with risk score, while 6 pathways were negatively correlated (Figure 10B).

CR-Derived Signature Was an Independent Index of the Prognostic Results of Prostate Cancer

Univariate and multivariate Cox analyses were executed to corroborate if such hallmark could

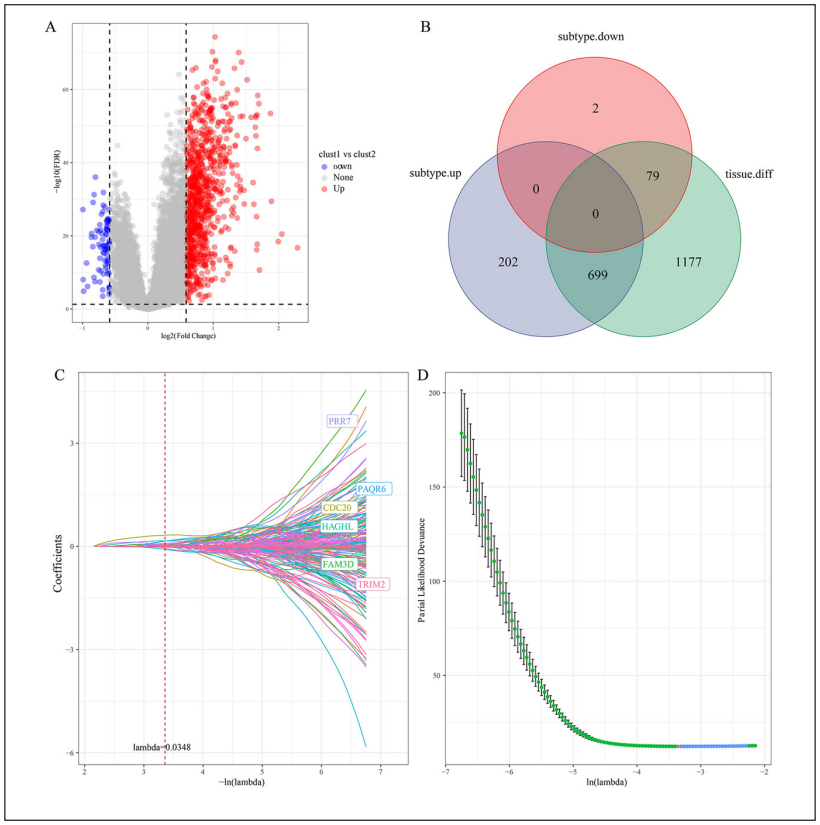

Figure 7. Establishment of signature. **A**, DEGs between 2 clusters in TCGA data set. **B**, Venn of differentially expressed genes and Tumorigenesis gene. **C**, LASSO coefficients profiles of 245 genes. **D**, LASSO regressive analysis with 10-fold cross-verification acquired 12 prognosis genes based on the minimal lambda value.

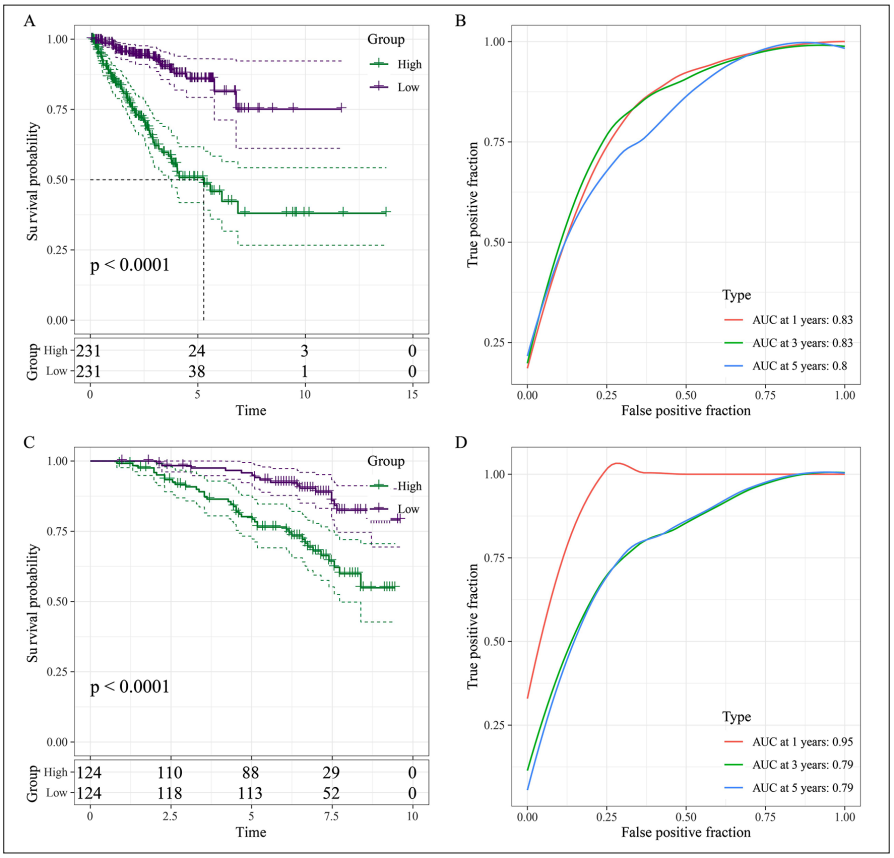

Figure 8. Prognostic analysis of signature. **A-B**, TCGA verifies the K-M and ROC curves of the data set. **C-D**, K-M and ROC curves of GSE116918 dataset.

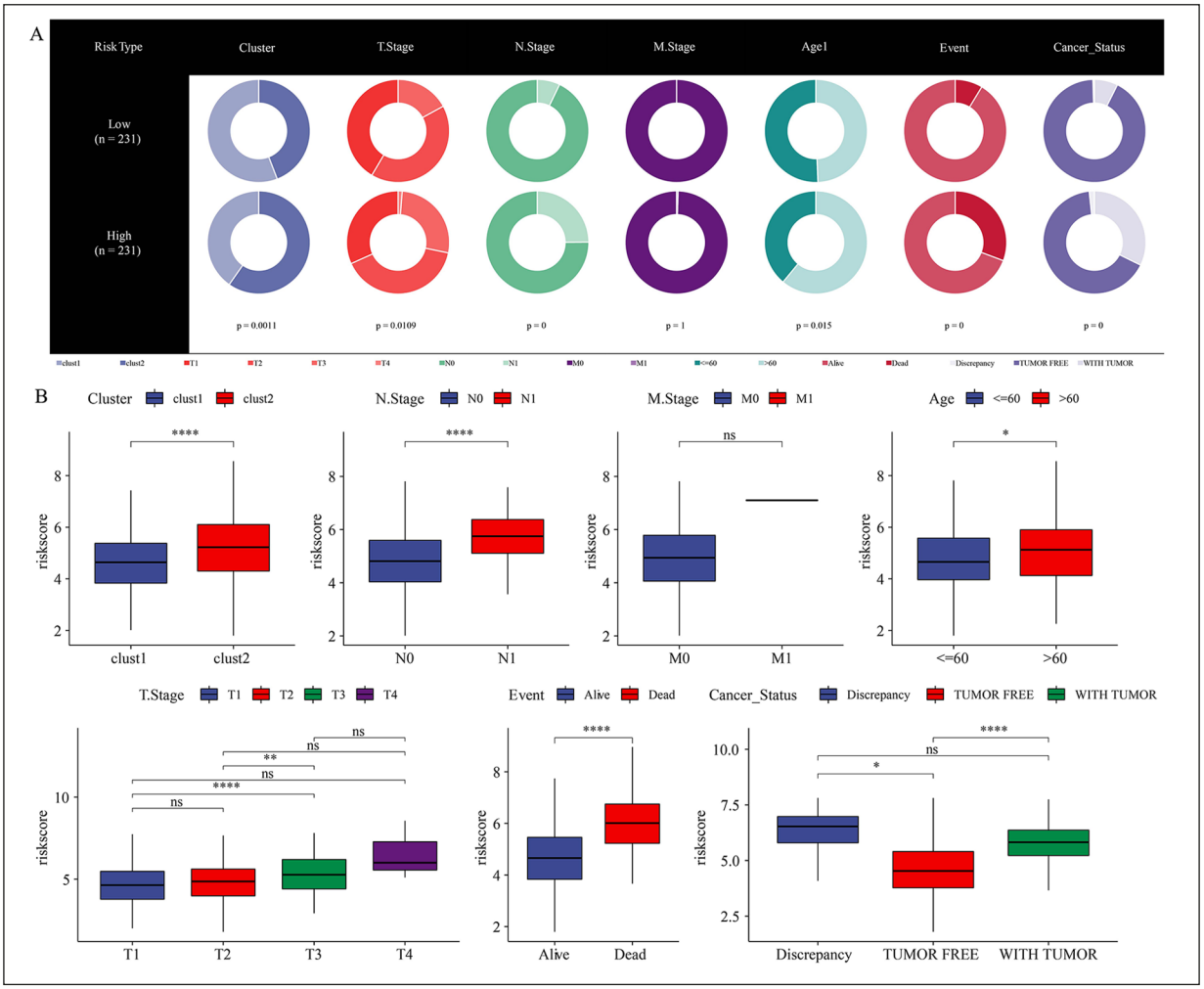

Figure 9. The distributional status of diverse clinical characteristics of $risk_{high}$ and $risk_{low}$ sufferers **A**, which involved Clusters, T staging, N staging, M staging, and Age, Event and cancer status (**B**). Chi-square test was conducted.

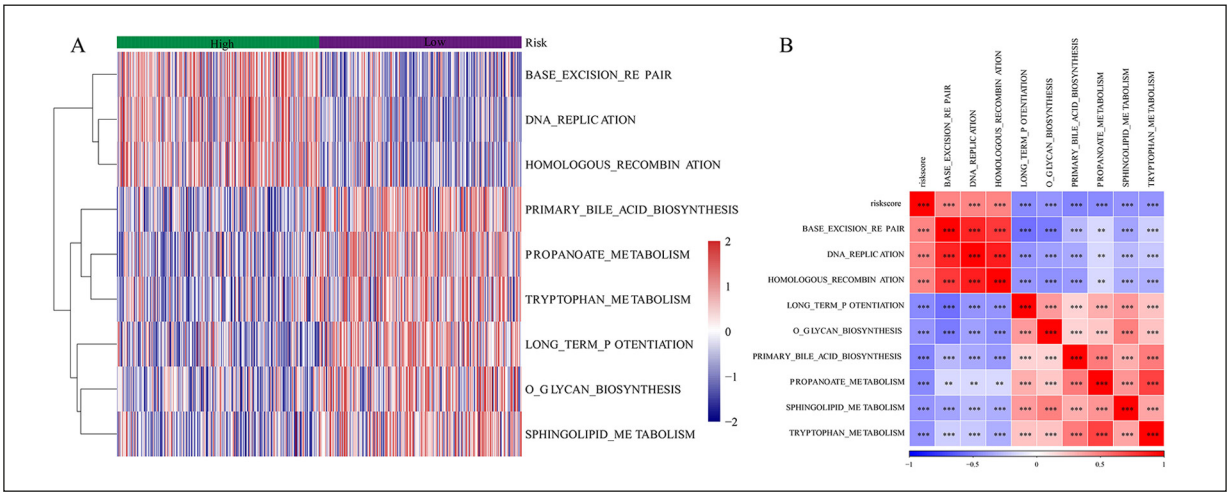

Figure 10. Functional enrichment analyses of $risk_{high}$ and $risk_{low}$ sufferers. **A**, Heatmap of significant pathway associated with risk scoring. **B**, Correlative analyses of pathways with risk scoring.

independently serve as a prognosis index. Univariable analyses revealed that T stage, N stage, Cluster and Risk type were evidently linked to the survival of prostate cancer sufferers (Figure 11A). Multivariable analyses revealed that T stage, Cluster and Risk type were evidently linked to prognoses (Figure 11B). Those outcomes unveiled that the CR-derived hallmark could independently serve as a prognosis index for prostate cancer sufferers.

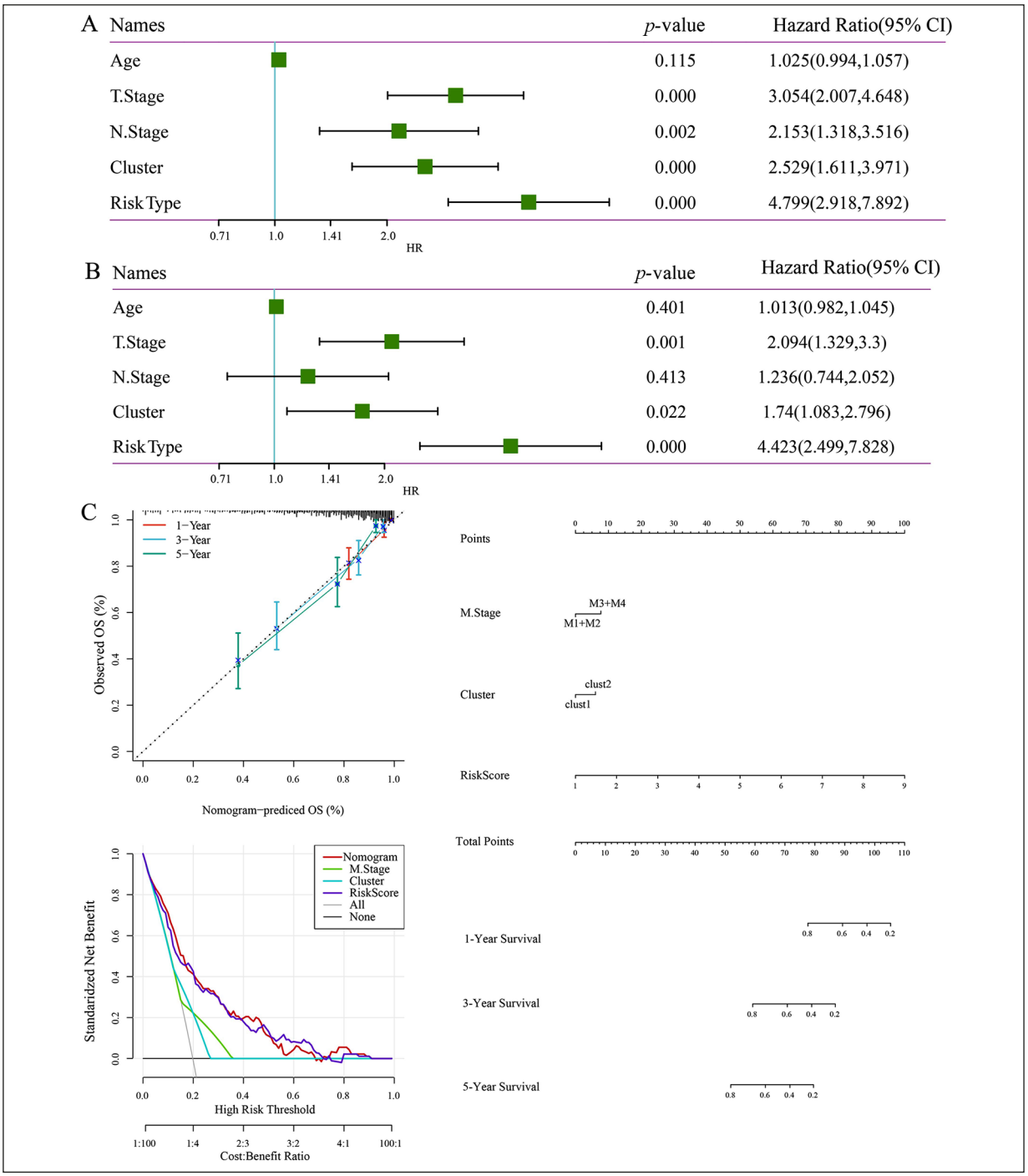

Figure 11. The hallmark could independently serve as a prognosis indicator. Univariable (**A**) and multivariable (**B**) Cox regressive analyses of risk scoring and clinical characteristics. **C**, Calibration for nomograph based on OS. DCA for assessing the ability of risk scoring, clusters, M staging and nomograph in forecasting prognoses. A nomograph on the basis of risk scoring and T staging for staging 1-, 3- and 5-year OS.

For the sake of predicting the survival of prostate cancer sufferers, our team developed a nomograph comprising T stage, cluster and risk scoring. Nomography predicted the 1-, 3-, 5-year OS of sufferers with prostate cancer (Figure 11C). The correction curve revealed that the actual OS of sufferers coincided with the forecasted results (Figure 11C). The nomogram had the favorable prediction ability (Figure 11C).

Immune Infiltration Level Analysis and Drug Sensitivity Analysis in CR-Based Signature

We also evaluated the speculated percentage of 22 immunocytes in $risk_{high}$ and $risk_{low}$ sufferers in the TCGA data set. 8 kinds of immunocytes with significantly different distributions between $risk_{high}$ and $risk_{low}$ sufferers (Figure 12A). Surprisingly, $risk_{high}$ sufferers had higher score of Stro-

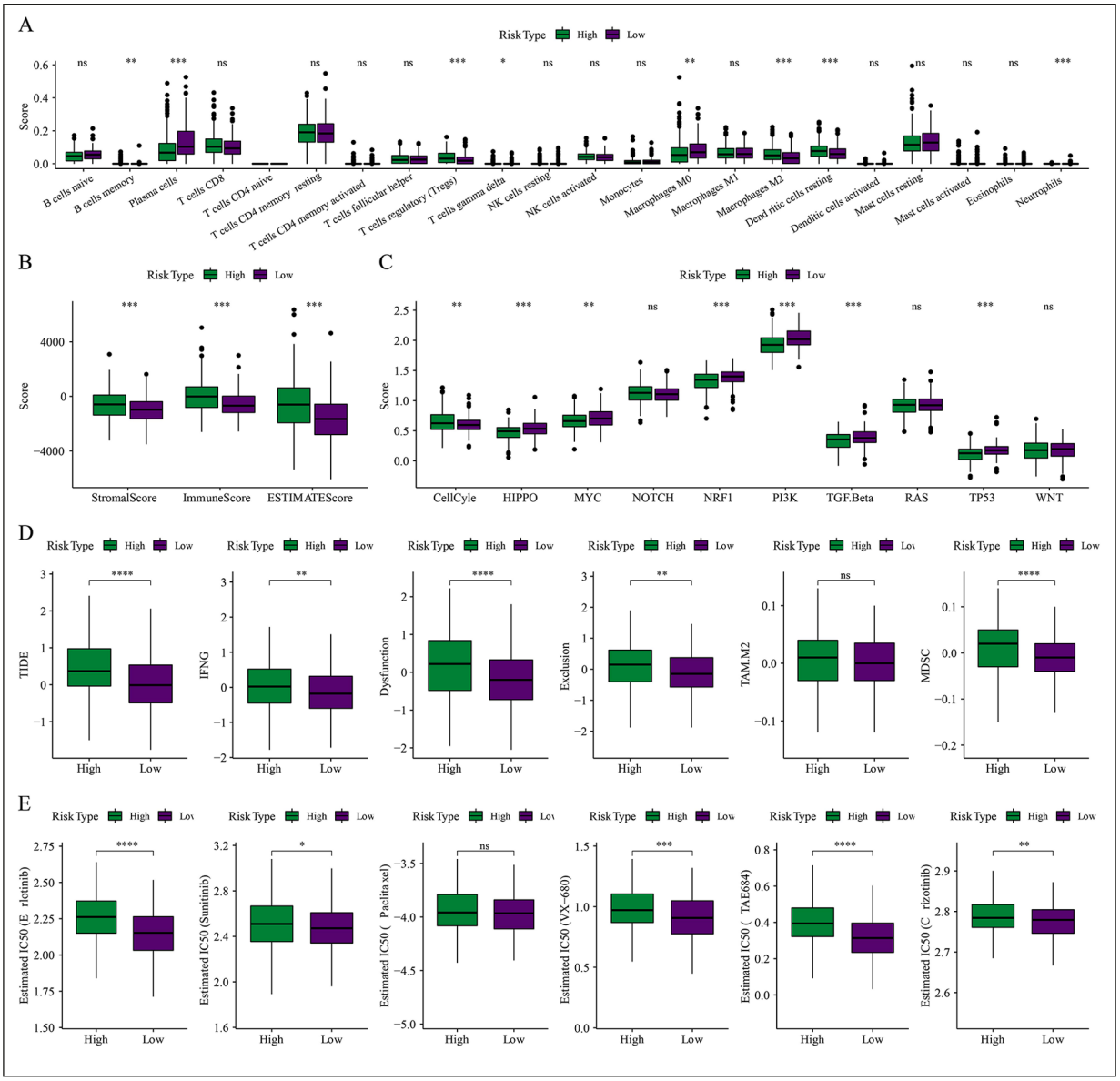

Figure 12. Characterization of tumor microenvironment and immunotherapy between $risk_{high}$ and $risk_{low}$ sufferers in TCGA dataset. **A**, Enrichment of 22 immunocytes assessed *via* CIBERSORT. **B**, ESTIMATE approach for computing stroma scoring and immunity scoring. **C**, Differences of 10 oncogenic pathways score between two clusters in TCGA dataset. **D**, TIDE scoring, IFNG scoring, T cell function disorder scoring, T cell exclusion scoring, MDSC and TAM.M2 scoring of $risk_{high}$ and $risk_{low}$ sufferers in TCGA data set. **E**, GDSC database analyses revealed that the IC50 results of medicines like erlotinib, sunitinib, paclitaxel, VX-680, TAE684 and crizotinib were greater in $risk_{high}$ sufferers in contrast to $risk_{low}$ sufferers.

malScore, ImmuneScore and ESTIMATEScore (Figure 12B). Our team then evaluated the 10 enriched oncogenesis pathways and discovered that 7 of 10 oncogenesis pathways were enriched in a differential manner between 2 clusters (Figure 12C).

Moreover, the forecasted scoring of immune therapy biomarkers was computed *via* the TIDE arithmetic. TIDE and IFNG were greater in $risk_{high}$ sufferers *vs.* $risk_{low}$ sufferers (Figure 12D). We evaluated the quality of TIDE T cell function disorder scoring, which also higher in $risk_{high}$ sufferers (Figure 12D). T cell exclusion and MDSC, except for TAM.M2, were all higher in $risk_{high}$ sufferers (Figure 12D). Those outcomes unveiled that $risk_{low}$ sufferers were better candidates for immunotherapy.

We also explored the susceptible diversity of commonly seen chemo medicines amongst these 2 groups. The outcomes revealed that the IC50 results of medicines like erlotinib, sunitinib, VX-680, TAE684 and crizotinib were greater in $risk_{high}$ sufferers *vs.* $risk_{low}$ sufferers, which unveiled that *vs.* $risk_{low}$ sufferers were remarkably more susceptible to those medicines (Figure 12E).

Discussion

In this study, 23 CRs with differential expression between prostate cancer tissues and normal tissues and associated with prognosis of prostate cancer were firstly screened from TCGA database. Based on 23 CRs, two molecular subtypes with significant prognostic differences, mutational status, and immune characteristics were identified. We then identified 10 CRs associated with prostate cancer prognosis by univariable and lasso Cox regressive analyses. Based on those 10 CRs, our team developed and corroborated a risk model related to prognoses. Survival analysis and ROC analysis show that the model has satisfactory prediction merit. Eventually, univariable and multivariable Cox analyses revealed that the risk scoring on the basis of 10 CRs independently serve as a prognosis index of prostate cancer. In addition, our team discovered that this marker was tightly associated with immunocyte infiltration and sensitive to a variety of chemotherapy drugs.

As a core part of the epigenetic mechanism, CRs regulate the transcriptional process of substantial cell genes, like oncogenes. Hence, their changed activity can greatly affect global genetic expression patterns and healthy cell signal transmission networks, facilitating the proliferative ability of oncogenes and eventual oncogenesis[23]. Largescale sequence identification research of mankind tumors' points to epigenetic modulators as hotspots for gene variants in gastric[24], liver[25], ovarian[26], prostate cancer[27], osteosarcoma[28], which highlights the significance of gene and epigenetic gatekeepers in the developmental process of tumor. Frequent mutations in genes encoding histones themselves in brain tumors further support the critical role of chromatin structure in tumorigenesis[29,30]. In this work, our team first identified 2 molecular subtypes of prostate cancer based on CRs and established a 10 CRs-signature.

FCER1A is capable of encoding an IgE acceptor, which is primarily expressed on the surfaces of mastocytes[31]. *FCER1A* has been discovered to participate in mammary carcinoma[32], glioma[33], *ZFP36L2*, zinc finger protein 36, C3H type-like 2 (called as Brf2, Erf2 and Tis11D, as well); it also has anti-cancer biofunction in multiple tumor types[34]. Overexpressed *ZFP36L2*/*TIS11D WT* gene suppressed the development of HeLa cells[35]. Consecutively, studies[36,37] have confirmed that Lysosomal protein transmembrane 4 beta (*LAPTM4B*) is aberrantly expressed in diverse malignancies and exerts an effect on tumor development. *LAPTM4B* is related to prostate cancer[38]. Evidence have suggested that the Tripartite motif-containing 2 (*TRIM2*) protein is related to oncogenesis effects in multiple malignant tumors, like lung adenocarcinoma[39], colonic and rectal carcinoma[40], and pancreatic cancer[41], *via* modulating cellular proliferative, metastatic, and transcriptional activities, as well as the ubiquitination route.

The expression of *SLC22A3* is significantly higher in colorectal cancer, and affects proliferation, migration, invasion, cell cycle and apoptosis[42]. *SCUBE2* increase suppressed the developmental process of cellular cycle, repressed cellular proliferative, metastatic, and invasive abilities, and it facilitates programmed cell death in breast cancer cells[43]. In prostate cancer cells, lipocalin-2 (*LCN2*) depletion induces attenuated proliferative ability, decreases expressing levels of proinflammation cell factors, lower adherence, and abnormal distributional status of F-actin[44]. Upregulated *PAQR6* is related to androgen receptor signal transmission and unsatisfactory prognoses in prostate carcinoma[45,46]. *CDC20* with its gene mutations are remarkably related to inferior survival of prostate cancer[47,48].

Limitations

Despite the fact that we used bio-informatics methods on a large sample to identify two genetic subgroups of prostate cancer with significant prognostic differences, as well as a 10 CRs-signature, we are required to note the limitations of our work. In the future, we plan to place a greater emphasis on research that is both fundamentally experimental and functionally in-depth. Other considerations were not taken into account on our end because the samples lacked essential clinical follow-up information, most notably diagnostic specifics, such as whether or not the patients had other health conditions, when differentiating the molecular sub-types.

Conclusions

In conclusion, we generated two subgroups and a 10 CRs signature based on CRs in order to guide tailored therapy for prostate cancer patients. CRs are vital for forecasting the prognostic results of prostate cancer sufferers and targeting CRs might be a valid strategy to treat prostate carcinoma. This research ought to be corroborated by more studies.

Conflict of Interest

All authors have completed the ICMJE uniform disclosure form. The authors have no conflicts of interest to declare.

Acknowledgements

None.

Funding

None.

Ethics Approval

Not Applicable.

References

1) Bray F, Ferlay J, Soerjomataram I, Siegel RL, Torre LA, Jemal A. Global cancer statistics 2018: GLOBOCAN estimates of incidence and mortality worldwide for 36 cancers in 185 countries. CA Cancer J Clin 2018; 68: 394-424.
2) Chang AJ, Autio KA, Roach M, 3rd, Scher HI. High-risk prostate cancer-classification and therapy. Nat Rev Clin Oncol 2014; 11: 308-323.
3) Bass EJ, Ahmed HU. Focal therapy in prostate cancer: A review of seven common controversies. Cancer Treat Rev 2016; 51: 27-34.
4) Xu T, Liu CL, Li T, Zhang YH, Zhao YH. LncRNA TUG1 aggravates the progression of prostate cancer and predicts the poor prognosis. Eur Rev Med Pharmacol Sci 2019; 23: 4698-4705.
5) Lu J, Xu J, Li J, Pan T, Bai J, Wang L, Jin X, Lin X, Zhang Y, Li Y, Sahni N, Li X. FACER: comprehensive molecular and functional characterization of epigenetic chromatin regulators. Nucleic Acids Res 2018; 46: 10019-10033.
6) Plass C, Pfister SM, Lindroth AM, Bogatyrova O, Claus R, Lichter P. Mutations in regulators of the epigenome and their connections to global chromatin patterns in cancer. Nat Rev Genet 2013; 14: 765-780.
7) Marazzi I, Greenbaum BD, Low DHP, Guccione E. Chromatin dependencies in cancer and inflammation. Nat Rev Mol Cell Biol 2018; 19: 245-261.
8) Li T, Yang J, Yang B, Zhao G, Lin H, Liu Q, Wang L, Wan Y, Jiang H. Ketamine Inhibits Ovarian Cancer Cell Growth by Regulating the lncRNA-PVT1/EZH2/p57 Axis. Front Genet 2020; 11: 597467.
9) Chen J, Wang F, Xu H, Xu L, Chen D, Wang J, Huang S, Wen Y, Fang L. Long Non-Coding RNA SNHG1 Regulates the Wnt/β-Catenin and PI3K/AKT/mTOR Signaling Pathways via EZH2 to Affect the Proliferation, Apoptosis, and Autophagy of Prostate Cancer Cell. Front Oncol 2020; 10: 552907.
10) Zhang X, Tao T, Liu C, Guan H, Huang Y, Xu B, Chen M. Downregulation of miR-195 promotes prostate cancer progression by targeting HMGA1. Oncol Rep 2016; 36: 376-382.
11) Wei JJ, Wu X, Peng Y, Shi G, Basturk O, Yang X, Daniels G, Osman I, Ouyang J, Hernando E, Pellicer A, Rhim JS, Melamed J, Lee P. Regulation of HMGA1 expression by microRNA-296 affects prostate cancer growth and invasion. Clin Cancer Res 2011; 17: 1297-1305.
12) Lee KH, Hong S, Kang M, Jeong CW, Ku JH, Kim HH, Kwak C. Histone demethylase KDM7A controls androgen receptor activity and tumor growth in prostate cancer. Int J Cancer 2018; 143: 2849-2861.
13) Yuan H, Han Y, Wang X, Li N, Liu Q, Yin Y, Wang H, Pan L, Li L, Song K, Qiu T, Pan Q, Chen Q, Zhang G, Zang Y, Tan M, Zhang J, Li Q, Wang X, Jiang J, Qin J. SETD2 Restricts Prostate Cancer Metastasis by Integrating EZH2 and AMPK Signaling Pathways. Cancer Cell 2020; 38: 350-365. e7.
14) Jager MJ, Brouwer NJ, Esmaeli B. The Cancer Genome Atlas Project: An Integrated Molecular View of Uveal Melanoma. Ophthalmology 2018; 125: 1139-1142.
15) Toro-Domínguez D, Martorell-Marugán J, López-Domínguez R, García-Moreno A, González-Rumayor V, Alarcón-Riquelme ME,

Carmona-Sáez P. ImaGEO: integrative gene expression meta-analysis from GEO database. Bioinformatics 2019; 35: 880-882.

16) Wilkerson MD, Hayes DN. ConsensusClusterPlus: a class discovery tool with confidence assessments and item tracking. Bioinformatics 2010; 26: 1572-1573.

17) Mayakonda A, Lin DC, Assenov Y, Plass C, Koeffler HP. Maftools: efficient and comprehensive analysis of somatic variants in cancer. Genome Res 2018; 28: 1747-1456.

18) Ito K, Murphy D. Application of ggplot2 to Pharmacometric Graphics. CPT Pharmacometrics Syst Pharmacol 2013; 2: e79.

19) Yang P, Chen W, Xu H, Yang J, Jiang J, Jiang Y, Xu G. Correlation of CCL8 expression with immune cell infiltration of skin cutaneous melanoma: potential as a prognostic indicator and therapeutic pathway. Cancer Cell Int 2021; 21: 635.

20) Fu J, Li K, Zhang W, Wan C, Zhang J, Jiang P, Liu XS. Large-scale public data reuse to model immunotherapy response and resistance. Genome Med 2020; 12: 21.

21) Jiang P, Gu S, Pan D, Fu J, Sahu A, Hu X, Li Z, Traugh N, Bu X, Li B, Liu J, Freeman GJ, Brown MA, Wucherpfennig KW, Liu XS. Signatures of T cell dysfunction and exclusion predict cancer immunotherapy response. Nat Med 2018; 24: 1550-1558.

22) Geeleher P, Cox N, Huang RS. pRRophetic: an R package for prediction of clinical chemotherapeutic response from tumor gene expression levels. PLoS One 2014; 9: e107468.

23) Shu XS, Li L, Tao Q. Chromatin regulators with tumor suppressor properties and their alterations in human cancers. Epigenomics 2012; 4: 537-549.

24) Zang ZJ, Cutcutache I, Poon SL, Zhang SL, McPherson JR, Tao J, Rajasegaran V, Heng HL, Deng N, Gan A, Lim KH, Ong CK, Huang D, Chin SY, Tan IB, Ng CC, Yu W, Wu Y, Lee M, Wu J, Poh D, Wan WK, Rha SY, So J, Salto-Tellez M, Yeoh KG, Wong WK, Zhu YJ, Futreal PA, Pang B, Ruan Y, Hillmer AM, Bertrand D, Nagarajan N, Rozen S, Teh BT, Tan P. Exome sequencing of gastric adenocarcinoma identifies recurrent somatic mutations in cell adhesion and chromatin remodeling genes. Nat Genet 2012; 44: 570-574.

25) Fujimoto A, Totoki Y, Abe T, Boroevich KA, Hosoda F, Nguyen HH, Aoki M, Hosono N, Kubo M, Miya F, Arai Y, Takahashi H, Shirakihara T, Nagasaki M, Shibuya T, Nakano K, Watanabe-Makino K, Tanaka H, Nakamura H, Kusuda J, Ojima H, Shimada K, Okusaka T, Ueno M, Shigekawa Y, Kawakami Y, Arihiro K, Ohdan H, Gotoh K, Ishikawa O, Ariizumi S, Yamamoto M, Yamada T, Chayama K, Kosuge T, Yamaue H, Kamatani N, Miyano S, Nakagama H, Nakamura Y, Tsunoda T, Shibata T, Nakagawa H. Whole-genome sequencing of liver cancers identifies etiological influences on mutation patterns and recurrent mutations in chromatin regulators. Nat Genet 2012; 44: 760-764.

26) Jones S, Wang TL, Shih Ie M, Mao TL, Nakayama K, Roden R, Glas R, Slamon D, Diaz LA, Jr., Vogelstein B, Kinzler KW, Velculescu VE, Papadopoulos N. Frequent mutations of chromatin remodeling gene ARID1A in ovarian clear cell carcinoma. Science 2010; 330: 228-231.

27) Zhao D, Cai L, Lu X, Liang X, Li J, Chen P, Ittmann M, Shang X, Jiang S, Li H, Meng C, Flores I, Song JH, Horner JW, Lan Z, Wu CJ, Li J, Chang Q, Chen KC, Wang G, Deng P, Spring DJ, Wang YA, DePinho RA. Chromatin Regulator CHD1 Remodels the Immunosuppressive Tumor Microenvironment in PTEN-Deficient Prostate Cancer. Cancer Discov 2020; 10: 1374-1387.

28) Zhang WB, Han FM, Liu LM, Jin HB, Yuan XY, Shang HS. Characterizing the critical role of metabolism in osteosarcoma based on establishing novel molecular subtypes. Eur Rev Med Pharmacol Sci 2022; 26: 2926-2943.

29) Wu G, Broniscer A, McEachron TA, Lu C, Paugh BS, Becksfort J, Qu C, Ding L, Huether R, Parker M, Zhang J, Gajjar A, Dyer MA, Mullighan CG, Gilbertson RJ, Mardis ER, Wilson RK, Downing JR, Ellison DW, Zhang J, Baker SJ. Somatic histone H3 alterations in pediatric diffuse intrinsic pontine gliomas and non-brainstem glioblastomas. Nat Genet 2012; 44: 251-253.

30) Schwartzentruber J, Korshunov A, Liu XY, Jones DT, Pfaff E, Jacob K, Sturm D, Fontebasso AM, Quang DA, Tönjes M, Hovestadt V, Albrecht S, Kool M, Nantel A, Konermann C, Lindroth A, Jäger N, Rausch T, Ryzhova M, Korbel JO, Hielscher T, Hauser P, Garami M, Klekner A, Bognar L, Ebinger M, Schuhmann MU, Scheurlen W, Pekrun A, Frühwald MC, Roggendorf W, Kramm C, Dürken M, Atkinson J, Lepage P, Montpetit A, Zakrzewska M, Zakrzewski K, Liberski PP, Dong Z, Siegel P, Kulozik AE, Zapatka M, Guha A, Malkin D, Felsberg J, Reifenberger G, von Deimling A, Ichimura K, Collins VP, Witt H, Milde T, Witt O, Zhang C, Castelo-Branco P, Lichter P, Faury D, Tabori U, Plass C, Majewski J, Pfister SM, Jabado N. Driver mutations in histone H3.3 and chromatin remodelling genes in paediatric glioblastoma. Nature 2012; 482: 226-231.

31) Bulfone-Paus S, Nilsson G, Draber P, Blank U, Levi-Schaffer F. Positive and Negative Signals in Mast Cell Activation. Trends Immunol 2017; 38: 657-667.

32) Lee JY, Park AK, Lee KM, Park SK, Han S, Han W, Noh DY, Yoo KY, Kim H, Chanock SJ, Rothman N, Kang D. Candidate gene approach evaluates association between innate immunity genes and breast cancer risk in Korean women. Carcinogenesis 2009; 30: 1528-1531.

33) Backes DM, Siddiq A, Cox DG, Calboli FC, Gaziano JM, Ma J, Stampfer M, Hunter DJ, Camargo CA, Michaud DS. Single-nucleotide polymorphisms of allergy-related genes and risk of adult glioma. J Neurooncol 2013; 113: 229-238.

34) Baou M, Jewell A, Murphy JJ. TIS11 family proteins and their roles in posttranscriptional gene

regulation. J Biomed Biotechnol 2009; 2009: 634520.

35) Iwanaga E, Nanri T, Mitsuya H, Asou N. Mutation in the RNA binding protein TIS11D/ZFP36L2 is associated with the pathogenesis of acute leukemia. Int J Oncol 2011; 38: 25-31.

36) Su Q, Luo H, Zhang M, Gao L, Zhao F. LAPTM4B promotes the progression of nasopharyngeal cancer. Bosn J Basic Med Sci 2021; 21: 305-312.

37) Rehman Z, Fahim A, Bhatti A, Sadia H, John P. Co-expression of HIF-1α, MDR1 and LAPTM4B in peripheral blood of solid tumors. PeerJ 2019; 7: e6309.

38) Zhang H, Wei Q, Liu R, Qi S, Liang P, Qi C, Wang A, Sheng B, Li L, Xu Y. Overexpression of LAPTM4B-35: a novel marker of poor prognosis of prostate cancer. PLoS One 2014; 9: e91069.

39) Lin Z, Lin X, Zhu L, Huang J, Huang Y. TRIM2 directly deubiquitinates and stabilizes Snail1 protein, mediating proliferation and metastasis of lung adenocarcinoma. Cancer Cell Int 2020; 20: 228.

40) Cao H, Fang Y, Liang Q, Wang J, Luo B, Zeng G, Zhang T, Jing X, Wang X. TRIM2 is a novel promoter of human colorectal cancer. Scand J Gastroenterol 2019; 54: 210-218.

41) Sun Q, Ye Z, Qin Y, Fan G, Ji S, Zhuo Q, Xu W, Liu W, Hu Q, Liu M, Zhang Z, Xu X, Yu X. Oncogenic function of TRIM2 in pancreatic cancer by activating ROS-related NRF2/ITGB7/FAK axis. Oncogene 2020; 39: 6572-6588.

42) Ren A, Sun S, Li S, Chen T, Shu Y, Du M, Zhu L. Genetic variants in SLC22A3 contribute to the susceptibility to colorectal cancer. Int J Cancer 2019; 145: 154-163.

43) Shen Y, Zhang M, Da L, Huang W, Zhang C. Circular RNA circ_SETD2 represses breast cancer progression via modulating the miR-155-5p/SCUBE2 axis. Open Med (Wars) 2020; 15: 940-953.

44) Schröder SK, Pinoé-Schmidt M, Weiskirchen R. Lipocalin-2 (LCN2) Deficiency Leads to Cellular Changes in Highly Metastatic Human Prostate Cancer Cell Line PC-3. Cells 2022; 11: 260.

45) Yang M, Li JC, Tao C, Wu S, Liu B, Shu Q, Li B, Zhu R. PAQR6 Upregulation Is Associated with AR Signaling and Unfavorite Prognosis in Prostate Cancers. Biomolecules 2021; 11:

46) Li B, Lin Z, Liang Q, Hu Y, Xu WF. PAQR6 Expression Enhancement Suggests a Worse Prognosis in Prostate Cancer Patients. Open Life Sci 2018; 13: 511-517.

47) Dai L, Song ZX, Wei DP, Zhang JD, Liang JQ, Wang BB, Ma WT, Li LY, Dang YL, Zhao L, Zhang LM, Zhao YM. CDC20 and PTTG1 are Important Biomarkers and Potential Therapeutic Targets for Metastatic Prostate Cancer. Adv Ther 2021; 38: 2973-2989.

48) Zhang Q, Huang H, Liu A, Li J, Liu C, Sun B, Chen L, Gao Y, Xu D, Su C. Cell division cycle 20 (CDC20) drives prostate cancer progression via stabilization of β-catenin in cancer stem-like cells. EBioMedicine 2019; 42: 397-407.